Supplementary Information

Deterministic Control of Surface Mounted Metal-Organic Frameworks Growth Orientation on Metallic and Insulating Surfaces

Tatiana P. Vello[a,b], Mathias Strauss[a], Carlos A. R. Costa[a], Cátia C.Corrêa[a], Carlos César B. Bufon[a,b,c,*]

[a] Brazilian Nanotechnology National Laboratory (LNNano), Brazilian Center for Research in Energy and Materials (CNPEM), Zip Code 13083-970, Campinas, Sao Paulo, Brazil

[b]Department of Physical Chemistry, Institute of Chemistry (IQ), UNICAMP, 13084-862, Campinas, SP, Brazil

[c]Postgraduate Program in Materials Science and Technology (POSMAT), São Paulo State University (UNESP), 17033-360 Bauru, SP, Brazil.

Scanning Electronic Microscopy (SEM)

The SEM images for a 20-cycle HKUST-1 film were grown on bare Au, and Au functionalized with SH-C6. The images below were obtained using a FEI Inspect F50 microscope, with the Everhart Thornley secondary electron detector. The samples were previously coated with a carbon film deposited by a sputtering technique. The use of SAM as an anchor to immobilize the SURMOF structures creates a well attached and homogenous covering when compared to the film grown directly onto a Au surface.

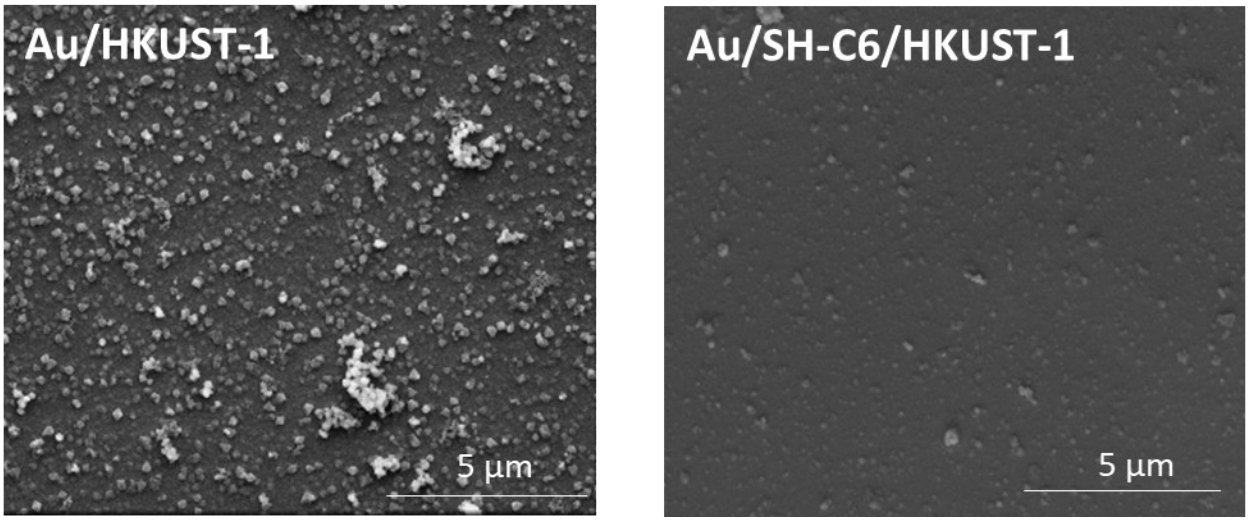

Figure S1. SEM images of a 20-cycle HKUST-1 film grown on bare Au (left), and on a functionalized-Au with the SAM SH-C6 (right) (20000x).

3D Laser Scanning Confocal Microscopy (LSCM)

Figure S2 exhibits 3D laser scanning confocal microscopy (LSCM, Keyence model VK-X200 series, Osaka, Japan) images. In Figure S2a (left), the HKUST-1 film grown on bare Au presented inferior adhesion to the substrate. Three different regions are identified in the sample (inset at right): a region where the film is partially delaminated (region 1), a region where the film is fully delaminated (region 2), and a region where the films remained intact on the surface (region 3). Figure S2b (left) shows the HKUST-1 film grown on Au functionalized with SH-C11. In this case (and also for Au substrates functionalized with SH-C3, SH-C6, SH-C11, and SH-C16), the film is homogeneous and well-attached to the surface. The roughnesses of the HKUST-1 films, shown in the inset of Figure S2b (right), are similar regardless of the SAMs chain length. The roughness is also lowered by using the SAM coverage when compared with the HKUST-1 films grown on bare Au.

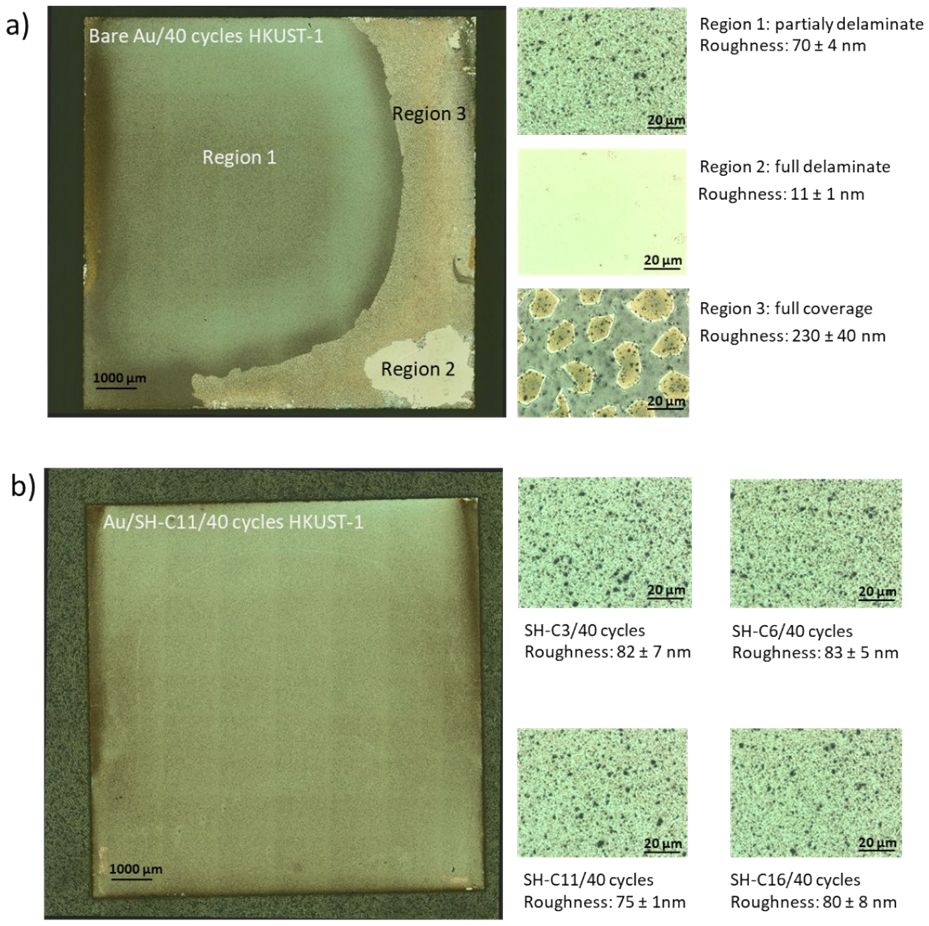

Figure S2. LSCM images for a 40-cycle HKUST-1 film grown onto (a) bare Au and (b) Au-functionalized with SAMs. The images forming the figure at the left were acquired using a 10x zoom mode. The inset images (right) were acquired using the 150x zoom mode.

Crystalline orientation as a function of the number of deposition cycles

The plots of full width at half maximum (FWHM) values of 222 and 400 peaks as a function of the number of deposition cycles (Figure S3) shows that pyramidal crystallites ([100] oriented) grow slightly faster than triangular ones ([111] oriented). The FWHM is directly associated with the crystal sizes using the Scheerer equation. Using the Scherrer equation, the size of [111] and [100] crystallites were calculate using (222) and (400) peaks, respectively. The values are shown in Table S1.

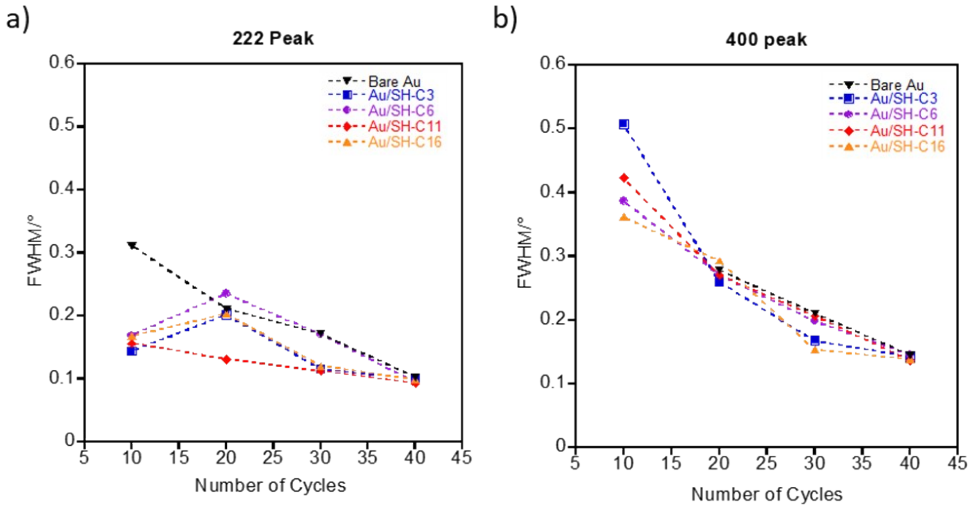

Figure S3. FWHM values of (222) and (444) peaks as a function of the number of deposition cycles.

Table S1. [111] and [100] crystallites size calculated by Scherrer equation using data from peaks (222) and (400), respectively.

Peak 222				
Cycles	SH-C3	SH-C6	SH-C11	SH-C16
10	55.7 nm	47.4 nm	51.2 nm	47.9 nm
20	39.8 nm	34.2 nm	61.3 nm	39.5 nm
30	69.4 nm	47.0 nm	71.7 nm	66.7 nm
40	80.9 nm	84.2 nm	86.3 nm	81.1 nm
Peak 400				
Cycles	SH-C3	SH-C6	SH-C11	SH-C16
10	15.9 nm	20.8 nm	19.0 nm	22.2 nm
20	31.0 nm	29.7 nm	29.7 nm	27.4 nm
30	47.9 nm	40.5 nm	39.0 nm	52.3 nm
40	56.6 nm	55.1 nm	58.7 nm	58.2 nm

Figure S4 exhibits the diffractograms of different depositions cycles of the HKUST-1 film. As shown in the figure, the [111] peaks of 5 and 10 cycles samples are more intense and sharper than [100] peaks. The [100] peaks start to increase from 20 cycles, becoming more intense and sharper than the [111] ones.

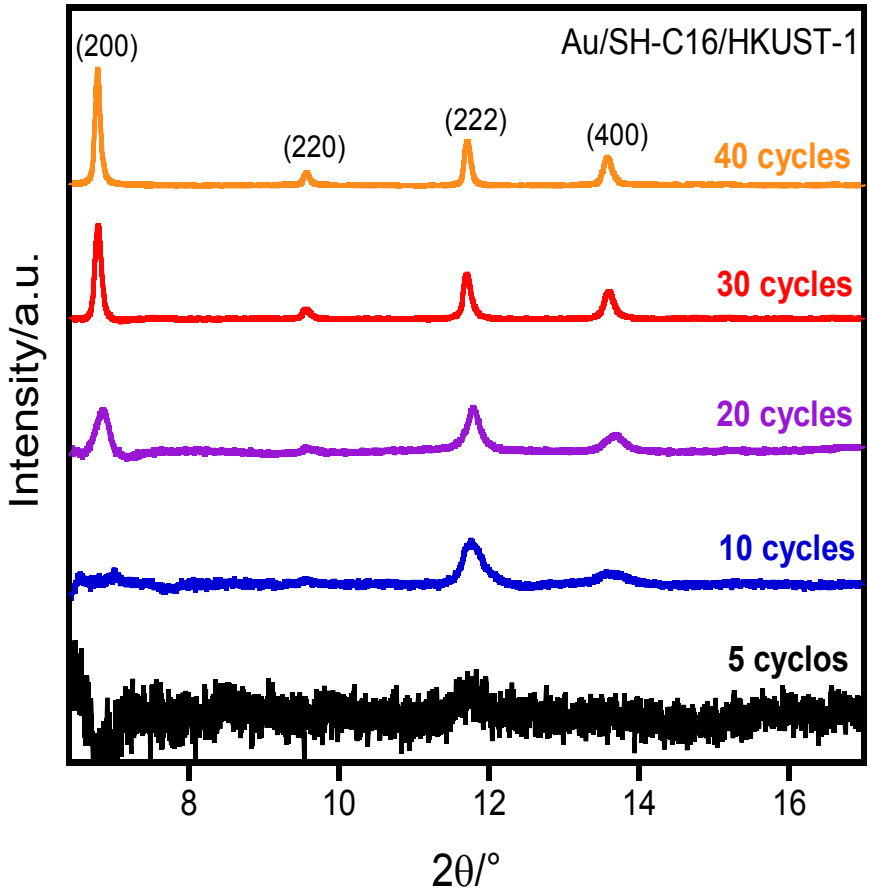

Figure S4. Diffractograms for Au/SH-C16-coated surfaces comprising HKUST-1 with different deposition cycles. The diffractogram data was normalized using the (222) peak intensity value.

Atomic force microscopy (AFM) images

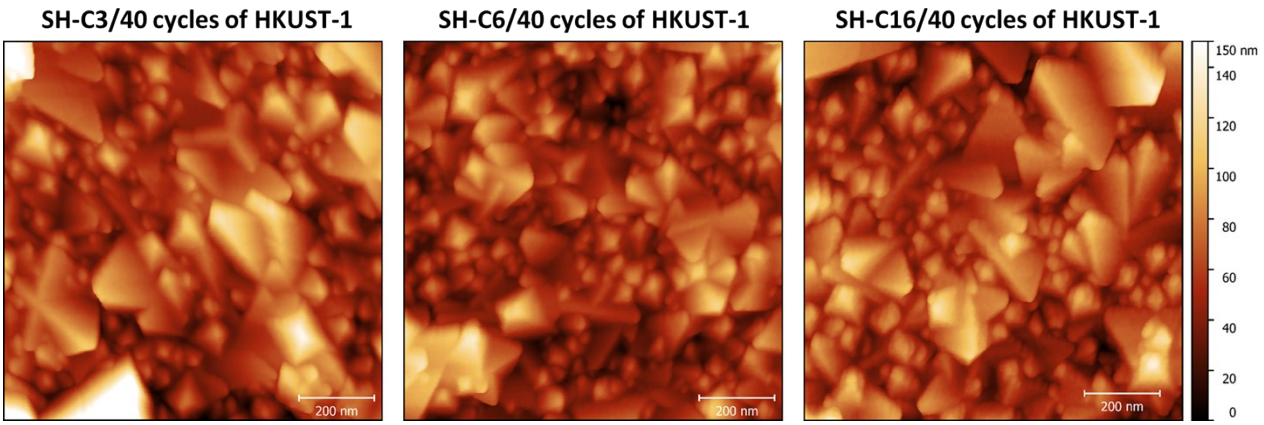

Figure S5:1x1 μm AFM image of Au functionalized with SH-C3, SH-C6, and SH-C16. The SURMOF is formed by a 40 cycle-HKUST-1 film.

Electrochemical characterization

The electrochemical measurements have been performed using a three-electrode cell connected to a potentiostat (AutoLab PGSTAT302N with FRA mode, Methrom). The cyclic voltammetry (Figure S6a) and the electrochemical impedance measurements (Figure S6b) were carried out with bare Au, and on Au functionalized with SAMs substrates. $[Fe(CN)4]^{3-/4-}$ was used as the redox probe. The voltammograms (Figure S6a) show that the suppression of current values and peak-to-peak separation (shown in Table S2) increases as the SAMs chain length increases. Also, the charge transfer resistance is observed higher for longer SAM chains. These responses indicate an incremental Au surface coverage as the number of carbons increases in the SAM's molecules.

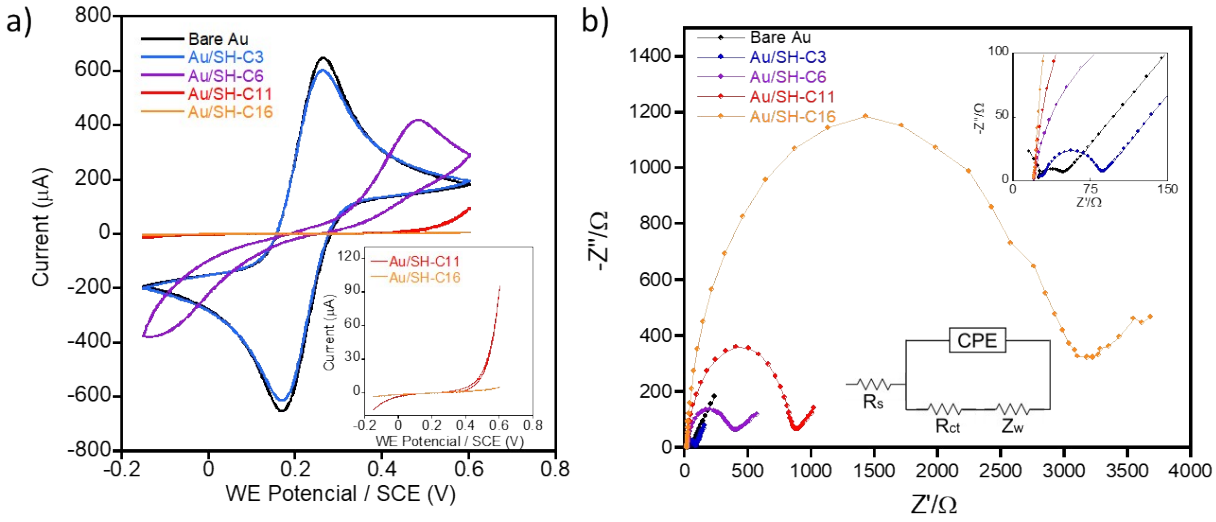

Figure S6. a)Voltammograms (scan rate of 30 mV/s) and b) electrochemical impedance (10 mV of AC Potential) of bare Au, and Au functionalized with SAMs in a 5 mM $[Fe(CN)_4]^{3-/4-}$ and 0.5 M KCl.

Table S2. Peak-to-peak voltage (ΔE_p), and charge transfer resistance (R_{ct}) for the bare Au and Au functionalized with SAMs.

Samples	ΔE_p (V)	R_{ct} (Ω)
Bare Au	100.8 mV	26
Au/SH-C3	90.7 mV	57
Au/SH-C6	609.6 mV	391
Au/SH-C11	-	857
Au/SH-C16	-	3346

X-ray Photoelectron Spectroscopy (XPS)

Table S3. XPS binding energy, full width at half maximum (FWHM), and atomic percentage values of carbon species of different samples (Au/SH-C3 and Au/SH-C16 with 0.5 cycles of HKUST-1).

SAM/0.5 cycle HKUST-1	Peak	Binding Energy/eV	FWHM/eV	Atomic abundance/%
SH-C3 Sample 1	C-C	284.6	1.3	64.9
	COOH	288.8	1.4	9.9
	C=O	287.6	1.0	13.4
	C-O	285.8	1.4	11.8
SH-C3 Sample 2	C-C	284.7	1.4	61.5
	COOH	288.9	1.5	10.0
	C=O	287.7	1.5	15.2
	C-O	286.0	1.5	13.3
SH-C3 Sample 3	C-C	284.7	1.4	61.9
	COOH	289.0	1.5	11.1
	C=O	287.7	1.5	14.0
	C-O	286.0	1.5	13.0

SAM/0.5 cycle HKUST-1	Peak	Binding Energy/eV	FWHM/eV	Atomic abundance/%
SH-C16 Sample 1	C-C	284.7	1.1	79.9
	COOH	288.5	1.3	8.2
	C=O	287.5	1.5	3.7
	C-O	285.6	1.2	8.2
SH-C16 Sample 2	C-C	284.7	1.3	82.0
	COOH	288.5	1.5	7.6
	C=O	287.1	1.5	3.6
	C-O	285.8	1.5	6.8
SH-C16 Sample 3	C-C	284.65	1.3	83.5
	COOH	288.43	1.4	6.7
	C=O	286.96	1.4	3.4
	C-O	285.78	1.4	6.5

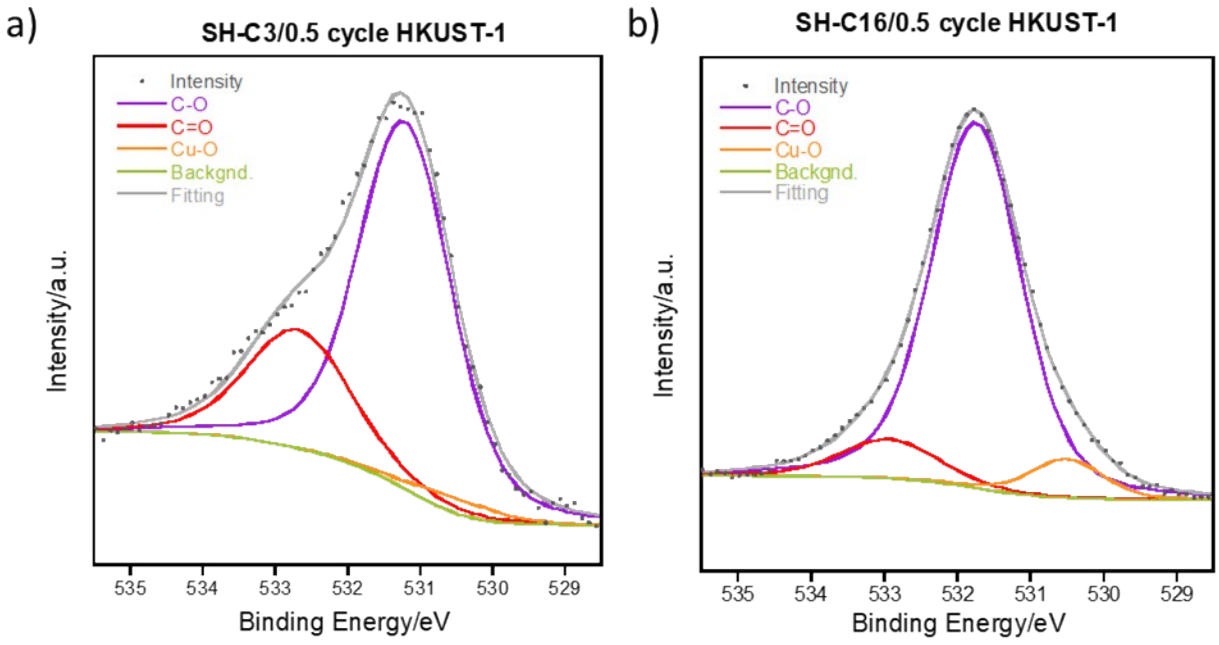

Figure S7. High-resolution XPS spectra at the oxygen region for Au/SH-C3 and Au/SH-C16 after immersion in copper acetate solution alone, to form 0.5 cycles.

Table S4. XPS binding energy, full width at half maximum (FWHM) and atomic percentage values of oxygen species for surfaces comprising of Au/SH-C3 and Au/SH-C16 with 0.5 cycles of HKUST-1

		Binding energy/eV	FWHM/eV	Atomic abundance/%
SH-C3/0.5 cycle HKUST-1	C-O	531.21	1.52	71.43
	C=O	532.69	1.71	25.66
	Cu-O	530.49	1.52	2.90
SH-C16/0.5 cycle HKUST-1	C-O	531.75	1.46	83.11
	C=O	532.94	1.57	9.67
	Cu-O	530.50	1.19	7.22

Figure S8 exhibits the high-resolution XPS spectra at the copper region for Au/SH-C3 and Au/SH-C16 after immersion in copper acetate solution alone (to form 0.5 cycles), and for a 10-cycles HKUST-1 film. The presence of peaks in the region between 960 to 928 eV indicates the presence of the Cu clusters on the surface after the exposition to the copper acetate solution. The binding energy values of Cu in the SH-C16 system are higher than the SH-C3 system, exhibiting a more electronegative bond of copper. In this case, when the SAM chain length changes from 3 to 16 carbons, the band shifts to values closer to the 10-cycle HKUST-1 SURMOF spectrum. Due to the high tendency of Cu-clusters to exhibit paddle-wheel arrangements on longer SAM/Cu-Ac interfaces, the binding energy becomes similar to the HKUST-1 film, which is mainly defined by the paddle-wheel binds of the Cu clusters.

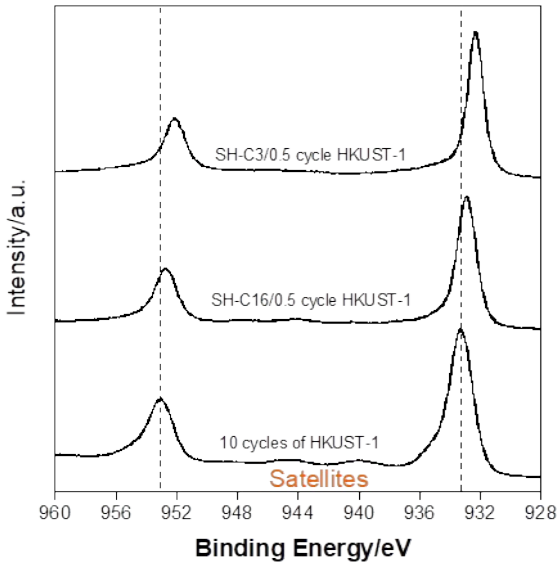

Figure S8: High-resolution XPS spectra at the copper region of Au/SH-C3 and Au/SH-C16 after immersion in copper acetate solution alone to form 0.5 cycles, and for 10-cycles HKUST-1 film.

Characterization of the growth of the HKUST-1 films on Al_2O_3 substracts

Figure S9 exhibits LSCM images of HKUST-1 films grown on bare Al_2O_3, and Al_2O_3 functionalized with PO-C11. On both surfaces, the HKUST-1 film shows high surface coverage and homogeneity. Figure S10 shows the AFM images Al_2O_3 functionalized with PO-C3, PO-C6, PO-C11 and PO-C16 with 40 cycle-HKUST-1 films deposited. Figure S11 exhibits the XPS data for the carbon region on samples consisting of Al_2O_3/PO-C3 and Al_2O_3/PO-C16 interfaces after immersion in Cu-Ac solution alone. The same behavior present for Au surfaces is exhibited on the Al_2O_3 ones. Thus, we can also extend the explanation of the SAMs/Cu-Ac cluster interface to the insulating surfaces. The Figure S12 exhibits AFM images of Au and Al_2O_3 with no SAM and functionalized with SAMs with short and long chains.

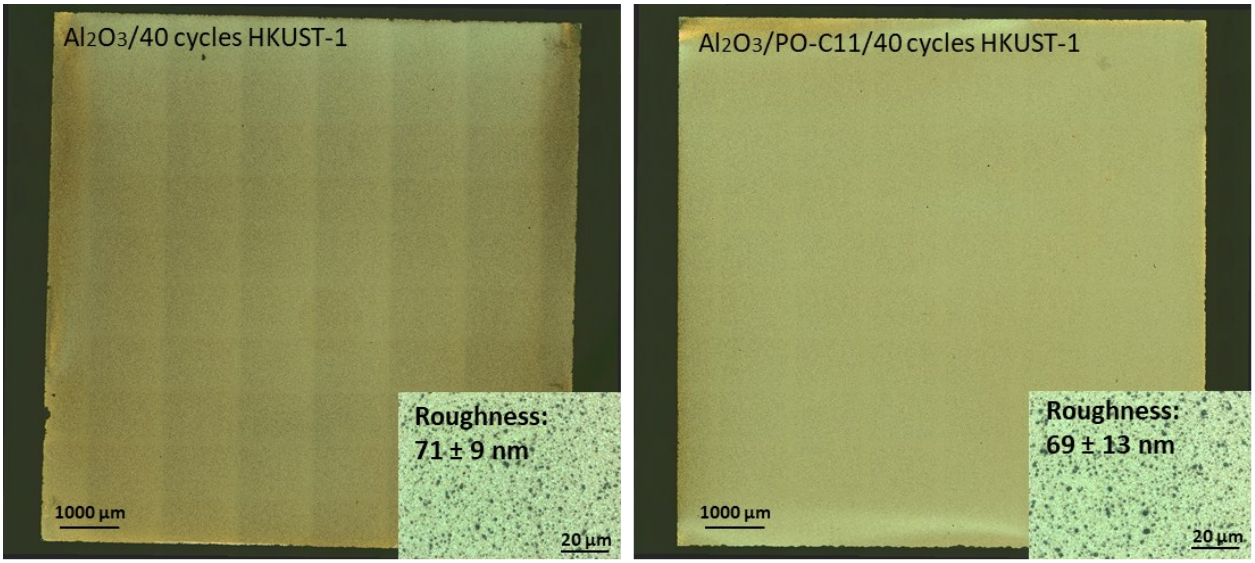

Figure S9. LSCM assembled images for a 40-cycle HKUST-1 film grown on bare Al_2O_3 (left) and Al_2O_3 functionalized with SAM PO-C11 (right). The images were acquired using a 10x zoom mode.

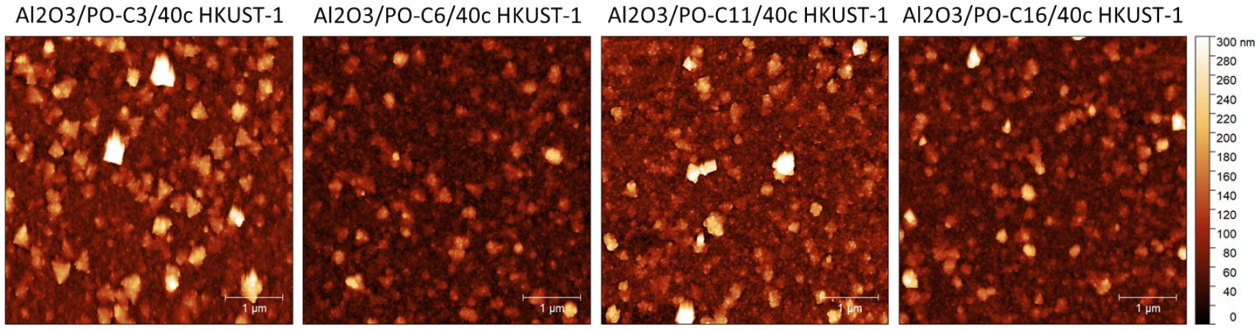

Figure S10. 5x5 µm AFM image of Al_2O_3 functionalized with PO-C3, PO-C6, PO-C11 and PO-C16 with 40 cycle-HKUST-1 films deposited.

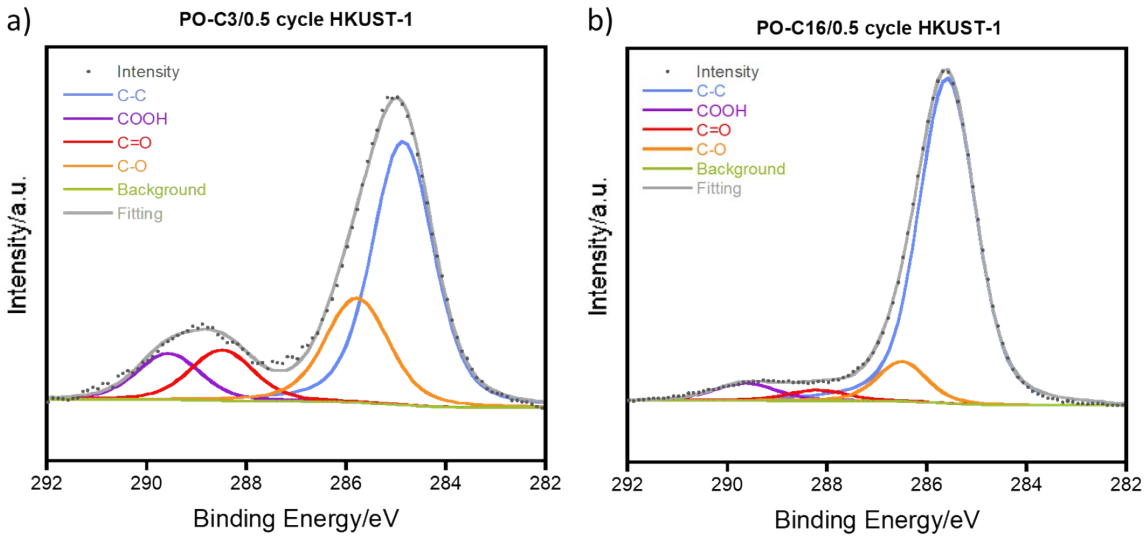

Figure S11. High-resolution XPS spectra at the carbon region for (a) Al_2O_3/PO-C3 and (b) Al_2O_3/PO-C16 interfaces after the immersion in Cu-Ac solution alone (0.5 cycles are formed).

Table S5. XPS binding energy, FWHM and atomic percentage values of oxygen species of Al_2O_3/PO-C3 and Al_2O_3/PO-C16 with 0.5 cycles of HKUST-1

		Binding energy/eV	FWHM/eV	Atomic abundance/%
PO-C3/0.5 cycle HKUST-1	C-C	284.87	1.46	55.83
	COOH	289.56	1.50	10.22
	C=O	288.49	1.50	11.11
	C-O	285.79	1.50	22.84
PO-C16/0.5 cycle HKUST-1	C-C	284.59	1.34	82.94
	COOH	288.65	1.50	5.05
	C=O	285.5	1.16	8.95
	C-O	287.19	1.50	3.06

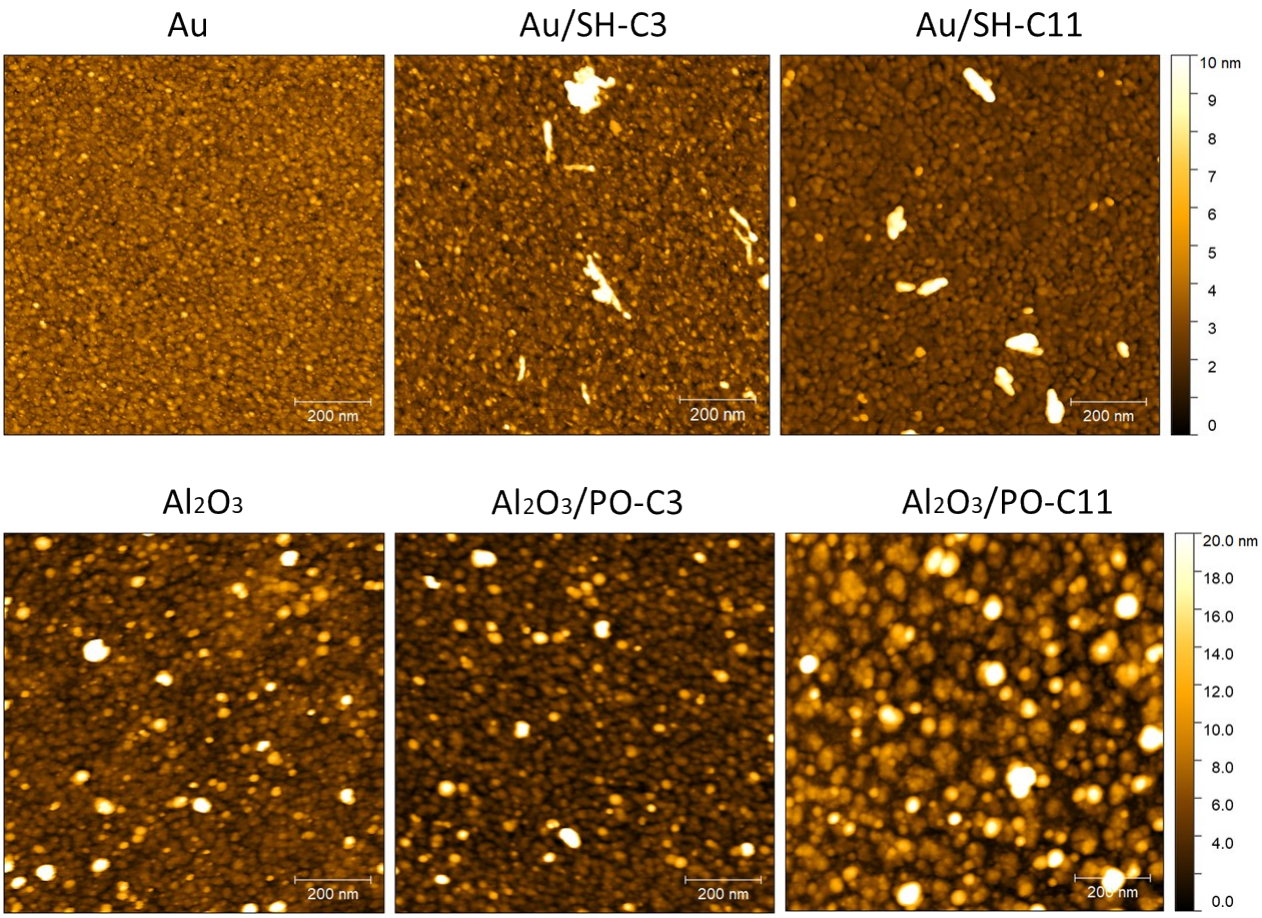

Figure S12.1x1 μm AFM images of Au and Al2O3 with no SAM and functionalized with SAMs with short and long chains.